# Methods for long-term GNSS clock offset prediction

Jaakko Pihlajasalo, Helena Leppäkoski,Saara Kuismanen, Simo Ali-Löytty, Robert Piché
Tampere University, Tampere, Finland
Email: {jaakko.pihlajasalo, helena.leppakoski, simo.ali-loytty, robert.piche}@tuni.fi
saara.kuismanen@here.com

***Abstract*—Clock offset predictions along with satellite orbit predictions are used in self-assisted GNSS to reduce the Time-to-First-Fix of a satellite positioning device. This paper compares three methods for predicting GNSS satellite clock offsets: polynomial regression, Kalman filtering and support vector machines (SVM). The regression polynomial and support vector machine model are trained from past offsets. The Kalman filter uses past offsets to estimate the clock offset coefficients. In tests with GPS and GLONASS data, it is found that all three methods significantly improve the clock predictions relative to extrapolation with the basic clock model of the last obtained broadcast ephemeris (BE). In particular, the 68% quantile of 7 day clock offset errors of GPS satellites was reduced by 66% with polynomial regression, 69% with Kalman filtering and 56% with SVM on average.**

## I. Introduction

A satellite positioning device needs the data of the broadcast navigation message from at least four satellites to compute the first position fix [1]. However receiving these messages can take at least 30 seconds, and much more in nonideal signal propagation conditions. In very harsh radio environment, it may happen that due to the signal attenuation or severe multipath, the receiver cannot demodulate the orbital and clock data at all. In addition, some low-energy IoT devices are not designed to perform the energy consuming data demodulation from GNSS signals. Assistance methods are used to reduce this Time-to-First-Fix (TTFF) or to recover from the inability to receive navigation data directly from the satellite signals[2]. With these methods, the device only needs to receive satellites' ranging signal; the orbital parameters and clock parameters it obtains some other way. One option is to download the parameters from a server. Then, methods such as real-time precise point positioning (PPP) [3] or assistance data from a provider of Secure User Plane Location (SUPL) services [4] can be used. Assistance provided over a network connection may however not be feasible, for example if Internet connection is unavailable or too expensive. Here we study the problem where we assume that no Internet connection is available or the user doesn't want to use it and the broadcast ephemeris (BE) is only occasionally available. In this case, the alternative is self-assisted ephemeris extension, where the broadcast parameters are computed on the device using prediction models applied to previously received broadcast data. This requires the prediction of both orbital and clock parameters over longer periods than the lifetime of the broadcast message. For applications like PPP, whose goal is accurate positioning, prediction is done over relatively short-term ranging from a few minutes up to 24 hours [5], [6], [7]. For improving the TTFF, accuracy requirements are less stringent but prediction is needed over much longer terms: typically up to two weeks for orbital parameters and four weeks for clock offsets. This study is concerned with the latter problem.

Both orbit and clock parameters need to be predicted, but this work will focus on clock offset predictions. In [8], methods for predicting GNSS satellites' orbit and clock offset are presented. The satellite's orbit is predicted by numerically integrating its equation of motion. In [9], Kalman filtering is used to estimate and predict the clock offset behaviour. In [10] and [11] more advanced methods for orbit prediction were presented, which motivates the study of more advanced models for clock offset prediction. These methods improve the orbit prediction enough for the error in clock prediction to be the dominating error in the user position estimate. This motivates further study of clock prediction methods for ephemeris extension. Increasing the time span over which clock prediction error is acceptably small also reduces the computational cost of the ephemeris extension system, because clock parameters won't need to be updated as often as the orbital parameters.

Atomic clocks aboard the satellite have synchronization errors with respect to the GNSS time scale, known as clock offsets. Some of the error in the clock offset is caused by the discretization of the data for bit allocation. Despite the accuracy of the atomic clocks aboard GNSS satellites, the clocks drift from GNSS time. The clocks aboard GNSS satellites are also affected by relativistic effects and by the age of the clocks. The navigation messages broadcast by satellites include the coefficients of polynomial models of the clock offset as a function of time [12]. Because the navigational messages are valid for only a few hours, a single set of coefficients is not accurate enough to be used for ephemeris extension, which needs predictions valid for days or even weeks. Thus different approaches for predicting the clock offsets are presented in this paper.

Clock offset prediction is basically a time series forecasting problem. In this paper, we propose three methods. One is an extension of the Kalman filter approach [9]; the others are polynomial regression and a support vector machine algorithm. Similar methods have been researched for real-time PPP. Polynomial fitting is used for the short-term prediction of the satellite clock offset for example in [5]. In [13] a Kalman

978-1-7281-2445-2/19/$31.00 

filtering solution for short-term predictions is studied. Least-squares support vector machine (LSSVM) approaches are studied in [6], [7]. The first paper uses LSSVM to predict clock bias up to 6 hours and the other uses a combination of polynomial fitting and LSSVM for predictions up to 24 hours. Both of the LSSVM methods use precise clock solutions as initial data. Methods are tested for GPS and GLONASS satellites, which cover different satellite generations, ages and clock types.

In the recent paper [14] various long-term prediction methods are presented. Their methods use precise clock products as the input data whereas we use broadcast data. We will compare the results of our methods with the results of their methods.

This article is structured as follows. In Section II the clock offset models and prediction methods are presented. In Section III the empirical testing setup and performance of the prediction methods are presented. In Section IV, we conclude the article.

## II. Clock models and prediction

In this section, we present the mathematical models we use in the extended prediction of the satellite clock offset.

### A. BE clock correction model

The GPS broadcast ephemeris message, updated every 2 hours, includes three coefficients for calculating clock offset. In Figure 1 are two examples of clock offset data behaviour. The clock offset $\tau$ at a time $t$ is described by a second order polynomial

$$\tau(t) = a_0 + a_1(t - t_{\text{toe}}) + a_2(t - t_{\text{toe}})^2, \tag{1}$$

where $t_{\text{toe}}$ is the time of ephemeris, i.e. the midpoint of the 4-hour validity interval of the BE. The coefficients $a_0$, $a_1$ and $a_2$ are called the offset, the frequency bias and frequency drift, respectively [12].

Broadcast messages of GLONASS satellites are updated every half hour, and include only two clock offset coefficients, $-a_0$ and $a_1$. The clock model is

$$\tau(t) = a_0 + a_1(t - t_{\text{toe}}). \tag{2}$$

Although it is not recommended, it is possible to use the polynomial (1) or (2) with the coefficients from the last obtained BE message to predict clock offsets beyond the time interval of validity. In the following, we refer to this practice as the *basic clock model*.

### B. Polynomial regression

If a set of $n$ BE messages collected over several days is available, a function can be fitted to them and used to predict future offsets. For GPS, we fit a second order polynomial of the form (1) with $t_{\text{toe}} = t_n$, which is the last collected BE. The linear regression model for fitting the polynomial model to the BE offsets is then

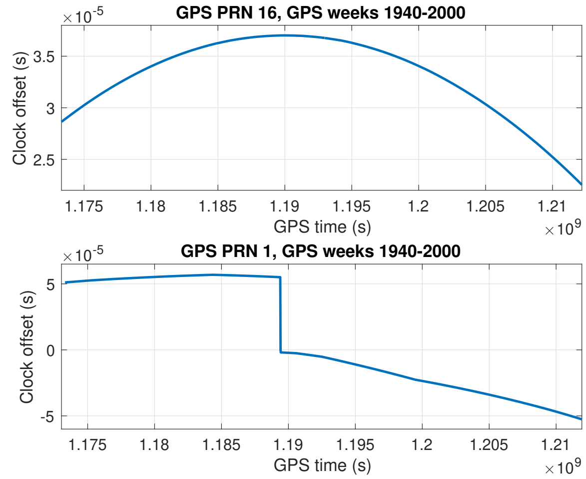


Fig. 1: Examples of clock offset behaviour as a function of time. In the upper figure we see regular behaviour and in the lower we see an example of a 50 ms jump in the data. A clock offset of 50 ms corresponds to 15 km offset in satellite position.

$$\begin{bmatrix}\tau(t_1)\\ \vdots \\ \tau(t_n)\end{bmatrix} = \begin{bmatrix}1 & t_1 - t_n & (t_1 - t_n)^2\\ \vdots & \vdots & \vdots\\ 1 & t_{n-1} - t_n & (t_{n-1} - t_n)^2\\ 1 & 0 & 0\end{bmatrix}\begin{bmatrix}a_0\\ a_1\\ a_2\end{bmatrix} + \begin{bmatrix}\varepsilon_1\\ \vdots\\ \varepsilon_n\end{bmatrix}, \tag{3}$$

where $t_i$ is the $t_{\text{toe}}$ of the $i$th BE message and $\varepsilon_i$ is random error.

Equation (3) can be expressed as

$$\boldsymbol{\tau} = \mathrm{X}\mathbf{a} + \boldsymbol{\varepsilon}. \tag{4}$$

The least squares solution [15, p. 121-122] of (4) is

$$\hat{\mathbf{a}} = (\mathrm{X}^T\mathrm{X})^{-1}\mathrm{X}^T\boldsymbol{\tau}. \tag{5}$$

For fitting we use BE messages that are 12 hours apart. For GLONASS, a first-order polynomial is fitted, because it fits the data about as well as a second-order polynomial. The fitting equation is obtained by omitting $a_2$ and the third column of X in (4).

### C. Kalman filter

A Kalman filter [15] can be used to reduce the noisiness of the broadcast clock parameters time series, as follows. The evolution of clock parameters is assumed to follow the polynomial models presented in section A. For GPS, the dynamic clock model has a state vector $x_k$ that consists of clock offset $\tau_k$, frequency bias $b_k$ and frequency drift $d_k$. The state evolution is written as

$$x_{k+1} = \begin{bmatrix}\tau_{k+1}\\ b_{k+1}\\ d_{k+1}\end{bmatrix} = \begin{bmatrix}1 & \Delta t_k & \frac{1}{2}\Delta t_k^2\\ 0 & 1 & \Delta t_k\\ 0 & 0 & 1\end{bmatrix}\begin{bmatrix}\tau_k\\ b_k\\ d_k\end{bmatrix} + w_k, \tag{6}$$

where $w_k$ is process noise, which is assumed to be white and normally distributed with zero mean and covariance matrix $Q_k$ [16]. $\Delta t_k$ is the time between $k+1$ and $k$th broadcast message updates. Similarly for GLONASS satellites the state evolution without frequency drift is

$$x_{k+1} = \begin{bmatrix} \tau_{k+1} \\ b_{k+1} \end{bmatrix} = \begin{bmatrix} 1 & \Delta \mathrm{t}_k \\ 0 & 1 \end{bmatrix} \begin{bmatrix} \tau_k \\ b_k \end{bmatrix} + w_k. \quad (7)$$

Covariance matrix $Q_k$ is obtained by the discretization of the stochastic differential equation of the clock evolution. We have simplified the model presented in [16] by assuming that all of the error in the state is caused by clock drift. This allows the model to have only one process noise parameter instead of three. Covariance matrix $Q_k$ for GPS satellites is

$$Q_k = q \begin{bmatrix} \frac{\Delta \mathrm{t}_k^5}{20} & \frac{\Delta \mathrm{t}_k^4}{8} & \frac{\Delta \mathrm{t}_k^3}{6} \\ \frac{\Delta \mathrm{t}_k^4}{8} & \frac{\Delta \mathrm{t}_k^3}{3} & \frac{\Delta \mathrm{t}_k^2}{2} \\ \frac{\Delta \mathrm{t}_k^3}{6} & \frac{\Delta \mathrm{t}_k^2}{2} & \Delta \mathrm{t}_k \end{bmatrix}, \quad (8)$$

where $q > 0$ is the process noise parameter. For GLONASS satellites the covariance matrix is

$$Q_k = q \begin{bmatrix} \frac{\Delta \mathrm{t}_k^3}{3} & \frac{\Delta \mathrm{t}_k^2}{2} \\ \frac{\Delta \mathrm{t}_k^2}{2} & \Delta \mathrm{t}_k \end{bmatrix}. \quad (9)$$

Details of the derivation of (9) are given in [16]; the derivation of (8) is similar.

The clock offsets from the broadcasts are treated as measurements. It is assumed that the BE clock offset values are not completely accurate. The measurement model for GPS is assumed to have the form

$$y_k = a_{0,k} = \begin{bmatrix} 1 & 0 & 0 \end{bmatrix} x_k + v_k, \quad (10)$$

where $v_k$ is the measurement noise, which is assumed to be white and normally distributed with zero mean and variance $R$. For GLONASS the measurement model is assumed to be

$$y_k = -a_{0,k} = \begin{bmatrix} 1 & 0 \end{bmatrix} x_k + v_k. \quad (11)$$

A Kalman filter based on these dynamic and measurement models is used to compute the posterior distribution of the clock parameters. The Kalman filter algorithm is described for example in [15, p. 217]. The initialization of the Kalman filter is done with the information filter [15, p. 239] for the first three steps, since initial covariance and frequency drift are not known.

Parameters $R$ and $q$ are chosen using historical broadcast ephemeris data and grid search. Parameters are optimized by predicting the clock using different combinations of parameters. Parameters with minimum prediction error are chosen for tests. These parameters can be different depending on the satellite, because of the different stability and age of the clocks. Two combinations of parameters were found the best for prediction with GPS satellites. For all of the satellites process noise parameter is $q = 10^{-47}$. Measurement noise variance is $R = 10^{-17}$ for about half of the satellites and $R = 10^{-18}$ for the rest. For all GLONASS satellites measurement noise variance is $R = 10^{-17}$ and process noise parameter $q$ varies from $10^{-38}$ to $10^{-31}$.

### D. Least squares support vector machine

Least squares support vector machines (LSSVM) are least squares solutions of the optimization problems in support vector machines. In LSSVM the solution to the optimization problem is found by solving a set of linear equations instead of solving a quadratic programming problem, as in standard SVMs. [17]

The input $\mathbf{t}$ of LSSVM is a set of $N$ reference ephemeris epoch times associated with clock offset parameter $a_0$ obtained from broadcast ephemeris data and the output set is the $a_0$ parameters. The time inputs are standardized with mean and standard deviation of the input values to make computation numerically stable. Clock offset is predicted with

$$\hat{a}_0(t) = \sum_{i=1}^{N} \alpha_i \mathrm{K}_\sigma(t, t_i) + b, \quad (12)$$

where $\hat{a}_0$ is estimate of clock offset at time $t$, $t_i$ is the $i$th input time and estimated parameters $\alpha$ and $b$ are from the LSSVM. $\mathrm{K}_\sigma(t, t_i)$ is the Gaussian kernel with scalar inputs defined as

$$\mathrm{K}_\sigma(t_i, t_j) = \exp\left(-\frac{(t_i - t_j)^2}{2\sigma^2}\right), \quad (13)$$

where $t_i$ and $t_j$ are standardized time stamps and $\sigma$ is a free parameter.

The training of the LSSVM is done as follows. Let the training set be $\{t_i, a_0(i)\}^N, i = 1, 2, \ldots, N$, where $N$ is number of training points, $t_i \in \mathbb{R}$ is input time and $a_0(i) \in \mathbb{R}$ is the BE clock offset at this time. The least squares formulation of the support vector machine problem is presented in [18]. The solution of the problem is given by

$$\begin{bmatrix} b \\ \boldsymbol{\alpha} \end{bmatrix} = \begin{bmatrix} 0 & \mathbf{1}_N^T \\ \mathbf{1}_N & \mathrm{K}_\sigma + c^{-1}\mathrm{I} \end{bmatrix}^{-1} \begin{bmatrix} 0 \\ \mathbf{a}_0 \end{bmatrix}, \quad (14)$$

where $\mathbf{a}_0$ is reference clock offset values and $\mathrm{K}_\sigma \in \mathbb{R}^{N \times N}$ is a kernel matrix with estimated $\sigma$ and elements $(\mathrm{K}_\sigma)_{i,j} = \mathrm{K}_\sigma(t_i, t_j)$ given by (13). This expression can be further simplified using matrix inversion formulas and algebra:

$$b = (\mathbf{1}_N^T(\mathrm{K}_\sigma + c^{-1}\mathrm{I})^{-1}\mathbf{1}_N)^{-1}\mathbf{1}_N^T(\mathrm{K}_\sigma + c^{-1}\mathrm{I})^{-1}\mathbf{a}_0 \quad (15)$$

$$\boldsymbol{\alpha} = (\mathrm{K}_\sigma + c^{-1}\mathrm{I})^{-1}(\mathbf{a}_0 - b\mathbf{1}_N). \quad (16)$$

Parameters $c$ and $\sigma$ are chosen in a similar way as with Kalman filter parameters. Search for both parameters is done with powers of ten. Parameters are constellation and satellite specific.

## III. Test setup and results

In this chapter, we explain the setup we used for our simulations and present the results of the presented methods for different GNSS constellations.

| PRN | Criterion (ns) | BE 3 days | BE 15 days | BE 30 days | Polynomial regression 3 days | Polynomial regression 15 days | Polynomial regression 30 days | KF 3 days | KF 15 days | KF 30 days | LS 3 days | LS 15 days | LS 30 days |
|---|---|---|---|---|---|---|---|---|---|---|---|---|---|
| 2 | RMS | 6.19 | 18.82 | 26.27 | 8.14 | 22.93 | 50.08 | 2.3 | 1.81 | 5.22 | 7.81 | 20.15 | 38.01 |
| | Range | 9.78 | 30.79 | 34.26 | 7.81 | 38.03 | 89.13 | 3.73 | 5.98 | 17.81 | 7.49 | 31.89 | 59.55 |
| 5 | RMS | 9.58 | 85.53 | 266.2 | 4.97 | 19.29 | 43.75 | 1.92 | 6.87 | 11.79 | 1.24 | 7.85 | 37.59 |
| | Range | 17.57 | 173.4 | 537.79 | 5.12 | 31.66 | 101.94 | 2.59 | 11.66 | 38.11 | 0.73 | 17.63 | 68.88 |
| 10 | RMS | 29.84 | 128.77 | 231.98 | 9.74 | 20.27 | 41.61 | **25.62** | **119.41** | **241.79** | 9.7 | 21.79 | 41.96 |
| | Range | 51.78 | 218.72 | 353.76 | 27.56 | 51.3 | 161.48 | **45.51** | **211.01** | **406.0** | 27.91 | 52.61 | 164.05 |
| 27 | RMS | 6.06 | 30.02 | 67.45 | 5.79 | 22.94 | 48.18 | 5.08 | 22.49 | 49.11 | 5.54 | 20.3 | 36.33 |
| | Range | 10.08 | 55.3 | 124.1 | 7.83 | 40.3 | 84.61 | 7.73 | 40.88 | 88.56 | 7.50 | 34.48 | 54.93 |

TABLE I: Table with results of individual predictions for four GPS satellites. Results are presented with RMS and range of predictions in nanoseconds for different prediction lengths and methods.

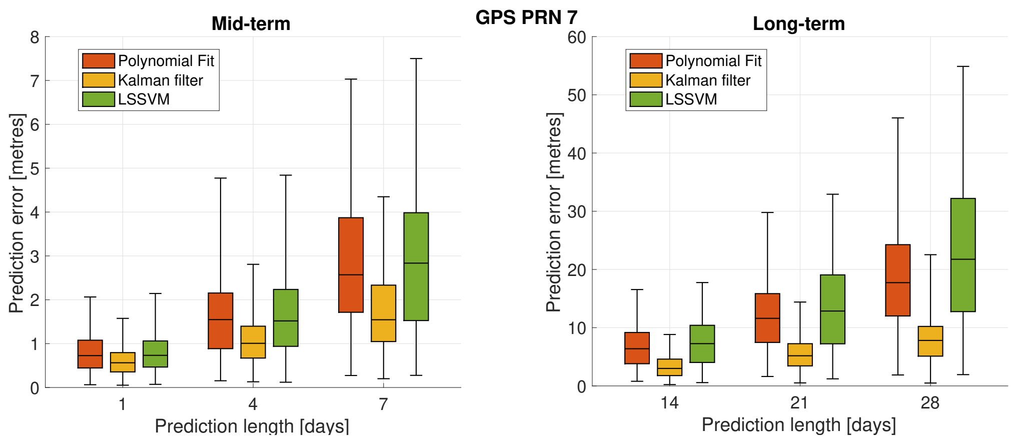


Fig. 2: Boxplots of quantiles of absolute error as a function of prediction length for GPS PRN 7 in meters with polynomial fit, Kalman filter and LSSVM. Prediction lengths are split in two figures to better present the mid-term separately from the long-term prediction. The upper and lower edges of the box show 68% and 32% quantiles respectively and the upper and lower whiskers show 95% and 5% quantiles respectively. The median error is shown by the line inside the box. Extrapolated last BE is not presented, to show the performance of other methods better. Extrapolated last BE has, for example 20.6 meter 68% quantile for 14 day prediction.

### A. *Testing setup*

We predict the satellite clock offset using broadcast ephemerides acquired from IGS products [19]. 28-day predictions are done with the basic clock model, regression polynomial, the clock model with Kalman filtered coefficients and the LSSVM. The latter three methods use data from 30 previous broadcasts 12 hours apart. Jumps in clock data, which cause large errors in prediction accuracy are omitted. If a jump in the clock data from BE is detected, the Kalman filter and the LSSVM are reset and predictions are not made until at least 30 new broadcasts are received. Because jumps are rare and easily detected, they can similarly be omitted in practical ephemeris extension system; there are almost always enough other satellites for successful TTFF reduction.

Predictions are made during GPS weeks 1940 to 2000 with equally spaced sampling instances, to match broadcast times. The Kalman filter is updated with every available broadcast while the regression polynomial and the LSSVM model are updated every sixth broadcast for convergence on a larger time interval. Non-equally spaced sampling instances would be better to simulate the real usage of a positioning device that in normal conditions doesn't receive new information every two hours. However having unequally spaced instances makes LSSVM parameter estimation more unstable. LSSVM and polynomial fitting are updated with the same ephemerides. Different fitting periods, the number of inputs and kernel functions can be an interesting research topic, but it is left for future work.

The accuracy of the clock predictions is assessed by comparing the predictions with broadcast ephemerides related to the predictions. Results are then presented as absolute error in meters instead of seconds to allow easy comparison with orbit prediction. For example, a two-week orbit prediction has about 25 meters of signal-in-space range error [11]. We also use 68% and 95% quantiles to show the results of the whole constellation.

| Method | Time (ms) |
|---|---|
| Polynomial fit | 0.095 |
| Kalman filter | 0.084 |
| LSSVM | 0.179 |

TABLE II: Average computation times of single prediction step for different methods.

In Table II we present average computation times of prediction steps for each method. Simulations were run with 64-bit Matlab (R2018a) on MacBook Pro version 10.12.6. From the table we can see that the LSSVM takes about twice the time for prediction compared with other methods.

### B. Results for GPS

For GPS, 31 of 32 satellites are available and only two of these satellites have Cesium clocks and the rest have Rubidium clocks [20]. The type of the clock affects the shape of the clock offset. Offsets of Cesium clocks have linear behaviour and the offset of Rubidium clocks have quadratic behaviour subject to time. Some of the satellites with Rubidium clocks have linear behaviour and will not be included in results. The broadcast data is received from the IGS [19].

Jumps, that were over 1 $\mu s$, in clock data were detected in some of the satellites. During these jumps a Notice Advisory to Navstar Users (NANU) warning is issued, but NANU messages are issued only a few days before the maintenance itself. Thus the message doesn't help if prediction is made before the warning is issued. A jump of 1 $\mu s$ in clock data corresponds to about 3 kilometers of error in satellite orbit prediction.

In the broadcast message of GPS satellites $a_2$ coefficient is usually set to zero which is sufficient for the 2 hour prediction window it's intended for. However, when predicting for a longer time period, the 2nd order polynomial coefficients computed by the Kalman filter are a better approximation of the frequency drift. Thus Kalman filter gives significantly better results than the basic clock model.

Generally, the performance of LSSVM is not good in comparison with simpler methods such as polynomial fit and Kalman filter. Kalman filter works well for most satellites, since rubidium clocks show a quadratic behaviour on the clock offset data, and thus the estimate of frequency drift is helpful. This estimate is also useful for detecting changes in clock data more accurately. Figure 2 shows the general results of the clock predictions with the presented methods. In general, the Kalman filter performed the best of the tested methods, with polynomial fit somewhat worse than the Kalman filter and LSSVM the worst.

In [14] Jigang et al. present and compare 7 methods for mid and long-term prediction. They presented results for four satellites with root mean square (RMS) error and range of individual predictions made at the start of the year 2015, for the prediction lengths of 1, 3, 15, 30 and 60 days. For comparison purposes we show results for prediction lengths 3, 15 and 30 days for the same time of ephemeris in Table I. Note that they use precise clock products for prediction and we use broadcast clock products which explains some of the difference between our and their methods. Results for our methods are in the same scope of error as their methods with the exception of PRN 10 with Kalman filter, which is in bold in the Table. With these individual predictions, LSSVM performs better than polynomial regression, but worse than KF. The results presented earlier in Figure 2 and in Table III include more satellites with more comprehensive tests. Testing with more satellites and initial time of ephemerides give better view of relative accuracies.

The parameter optimization of LSSVM is sensitive to changes which causes some of the errors of the model. The same parameter values won't last for long and should be updated biannually or after a jump is detected.

### C. Results for GLONASS

GLONASS has 24 available satellites from the same testing period as for GPS. Most GLONASS satellites have Cesium clocks, which have approximately linear behaviour of clock offset data. Despite having Cesium clocks, some of the clock offsets have quadratic behaviour. Again, jumps in clock data have been removed from the results to show general performance.

For some GLONASS satellites, the frequency bias coefficient has been set to zero, which causes high errors with the basic model for longer prediction intervals. The frequency bias given in broadcast message is sufficient for thirty minute intervals, but the Kalman filter again gets better results than the basic clock model for longer prediction lengths. The general results of GLONASS clock prediction can be seen in Figure 3 and Table III.

All of the methods improve the prediction accuracy almost the same amount on average. Kalman filter performs the best of the tested methods. Most of the GLONASS satellites have linear trend in clock offset data, thus the nonlinear model of LSSVM was expected to perform worse, but surpassed expectations by getting similar results as other methods.

## IV. Conclusions

In this paper, we presented three methods of predicting the clock offset of GPS and GLONASS satellites. Our results show that the basic clock model can be improved on with different methods. Kalman filter is computationally efficient and for an update requires the newest BE and state of the previous step. LSSVM is more inefficient in computation time and requires 30 previously received BEs for an estimate. LSSVM also gets worse results than a polynomial fit of the same input points for GPS satellites. LSSVM could possibly be better for interpolation tasks, instead of extrapolation. All three methods improve accuracy from the basic clock model for most GPS and GLONASS satellites. Further research is needed for the inclusion of other GNSS constellations.

## References


[1] "Global Positioning Systems Directorate Systems Engineering Integration Interface Specification IS-GPS-200," Tech. Rep., 4 2018, [Online]. Available: https://www.gps.gov/technical/icwg/IS-GPS-200J.pdf.

[2] Ivan G. Petrovski, *GPS, GLONASS, Galileo, and BeiDou for Mobile Devices - From Instant to Precise Positioning*. Cambridge University Press, 2014, doi: 10.1017/CBO9781139565455.

[3] G. Lachapelle, M. Petovello, Y. Gao, and L. Garin, "Precise point positioning and its challenges, aided-GNSS and signal tracking," *Inside GNSS*, vol. 1, pp. 16–21, 1 2006.

[4] "Secure user plane location architecture," Open Mobile Alliance, Tech. Rep., 4 2012, version 2.0, OMA-AD-SUPL-V2_0-20120417-A.

[5] H. Li, X. Liao, B. Li, and L. Yang, "Modeling of the gps satellite clock error and its performance evaluation in precise point positioning," *Advances in Space Research*, vol. 62, 5 2018, doi: 10.1016/j.asr.2018.05.025.

| Constellation | Prediction length (days) | Extrapolate last BE | Polynomial fit | | Kalman filter | | LSSVM | |
|---|---|---|---|---|---|---|---|---|
| | | Error (m) | Error (m) | Improvement (%) | Error (m) | Improvement (%) | Error (m) | Improvement (%) |
| GPS | 1 | 1.27 | 0.93 | 25.9 | 0.87 | 38.8 | 1.56 | -0.17 |
| | 4 | 5.86 | 1.95 | 61.8 | 2.14 | 63.4 | 2.92 | 48.4 |
| | 7 | 12.4 | 3.33 | 65.8 | 3.41 | 68.7 | 4.63 | 55.7 |
| | 14 | 37.0 | 7.55 | 67.2 | 6.66 | 74.6 | 10.1 | 60.0 |
| | 21 | 75.4 | 13.6 | 66.4 | 10.5 | 77.8 | 18.1 | 60.0 |
| | 28 | 128 | 21.4 | 65.5 | 15.3 | 79.4 | 28.3 | 60.8 |
| GLONASS | 1 | 16.6 | 3.54 | 74.9 | 3.52 | 76.4 | 4.31 | 69.5 |
| | 4 | 67.7 | 5.71 | 89.7 | 5.61 | 90.2 | 6.42 | 88.4 |
| | 7 | 119 | 8.05 | 91.5 | 7.79 | 92.1 | 8.56 | 90.9 |
| | 14 | 238 | 14.8 | 92.0 | 14.3 | 92.6 | 14.9 | 91.9 |
| | 21 | 358 | 22.7 | 91.9 | 22.1 | 92.2 | 22.5 | 91.8 |
| | 28 | 477 | 32.4 | 91.3 | 31.2 | 91.6 | 31.7 | 91.3 |

TABLE III: Table with average results of GPS and GLONASS satellites presented for different prediction lengths. Average of different satellites' 68% quantile are shown. Improvement means percentual change related to basic model (i.e. extrapolation of last BE).

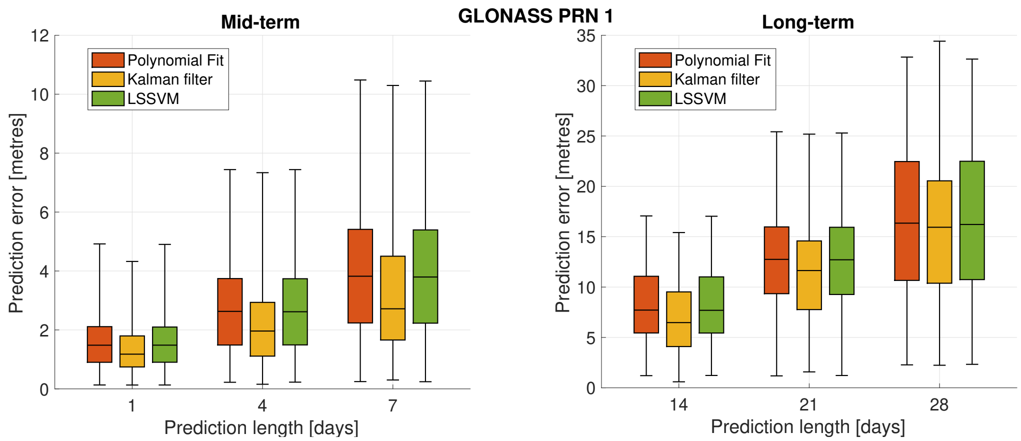


Fig. 3: Quantiles of absolute error for GLONASS PRN 1 in meters, with polynomial fit, Kalman filter and LSSVM. Prediction lengths are split in two figures to better present the mid-term separately from the long-term prediction. Box plot quantiles are as in Figure 2. Extrapolated last BE is not presented, to show performance of other methods better. Extrapolated last BE has, for example 287 meter 68% quantile for 14 day prediction.


[6] L. Jiye, C. Xihong, L. Qiang, and S. Jizhe, "Prediction of satellite clock errors using ls-svm optimized by improved artificial fish swarm algorithm," in *2013 IEEE International Conference on Signal Processing, Communication and Computing (ICSPCC 2013)*, Aug 2013, pp. 1–5, doi:10.1109/ICSPCC.2013.6664130.

[7] Y. Lei, Z. Hu, and D. Zhao, "A novel method for navigation satellite clock bias prediction considering stochastic variation behavior," in *China Satellite Navigation Conference (CSNC) 2014 Proceedings: Volume III*, J. Sun, W. Jiao, H. Wu, and M. Lu, Eds. Berlin, Heidelberg: Springer Berlin Heidelberg, 2014, pp. 369–379.

[8] M. Seppänen, J. Ala-Luhtala, R. Piché, S. Martikainen, and S. Ali-Löytty, "Autonomous prediction of GPS and GLONASS satellite orbits," *NAVIGATION*, vol. 59, no. 2, pp. 119–134, 2012, doi: 10.1002/navi.10.

[9] S. Martikainen, R. Piché, and S. Ali-Löytty, "Outlier-robust estimation of GPS satellite clock offsets," in *Localization and GNSS (ICL-GNSS), 2012 International Conference on*, Starnberg, Germany, 6 2012, pp. 1–5, doi: 10.1109/ICL-GNSS.2012.6253107.

[10] S. Rautalin, S. Ali-Löytty, and R. Piché, "Latent force models in autonomous GNSS satellite orbit prediction," in *2017 International Conference on Localization and GNSS*, 2017.

[11] J. Pihlajasalo, H. Leppäkoski, S. Ali-Löytty, and R. Piché, "Improvement of GPS and BeiDou extended orbit predictions with CNNs," in *26th European Navigation Conference, ENC 2018*. IEEE, 8 2018, pp. 54–59, doi: 10.1109/EURONAV.2018.8433244.

[12] M. J. Sanz Subirana, J.M. Juan Zornoza, *Clock Modelling*, European Space Agency, 2011, [Online]. Available: https://gssc.esa.int/navipedia/index.php/Clock Modelling.

[13] G. Huang and Q. Zhang, "Real-time estimation of satellite clock offset using adaptively robust kalman filter with classified adaptive factors," *GPS Solutions*, vol. 16, no. 4, pp. 531–539, Oct 2012, doi: 10.1007/s10291-012-0254-z. [Online]. Available: https://doi.org/10.1007/s10291-012-0254-z

[14] J. Lu, C. Zhang, Y. Zheng, and R. Wang, "Fusion-based satellite clock bias prediction considering characteristics and fitted residue," *Journal of Navigation*, vol. 71, no. 4, p. 955–970, 2018, doi:10.1017/S0373463317001035.

[15] P. S. Maybeck, *Stochastic Models, Estimation and Control, volume 1*. Academic Press, 1979.

[16] L. Galleani, "A tutorial on the two-state model of the atomic clock noise," *Metrologia*, vol. 45, no. 6, p. S175, 2008, doi: 10.1088/0026-1394/45/6/S23. [Online]. Available: http://stacks.iop.org/0026-1394/45/i=6/a=S23

[17] J. Suykens and J. Vandewalle, "Least squares support vector machine classifiers," *Neural Processing Letters*, vol. 9, pp. 293–300, 6 1999, doi: 10.1023/A:101862860.

[18] H.-Q. Wang, F.-C. Sun, Y.-N. Cai, L.-G. Ding, and N. Chen, "An unbiased LSSVM model for classification and regression," *Soft Computing*, vol. 14, no. 2, pp. 171–180, 1 2010, doi: 10.1007/s00500-009-0435-z.

[19] "IGS Products," [Online]. Available: http://www.igs.org/products.

[20] "GPS OPERATIONAL SATELLITES (BLOCK II/IIA/IIR/IIR-M/IIF)," United States Naval Observatory, Tech. Rep., 2018, [Online]. Available: ftp://tycho.usno.navy.mil/pub/gps/gpsb2.txt.